Supplementary Figures

Supplementary Figure Legends

Supplementary Figure 1. Triple negative breast cancer cells respond variously to PI3Kα inhibitor Alpelisib, with hyperphosphorylated AKT as a critical biomarker for cancer resistance by PTEN loss

(a) Colony-formation assay of HCC-1806, HCC-1937, SUM-159, MDA-MB-157, MDA-MB-231, MDA-MB-468, BT-549, Hs-578t, and HMEC cells treated with Alpelisib (1 μM).

(b) Representative flow cytometry analysis (annexin V+, 7AAD−) of HCC-1806, HCC-1937, MDA-MB-231, MDA-MB-468 treated with Alpelisib (1 μM).

(c) The percentage of apoptotic cells determined by flow cytometry analysis after treatment of control or Alpelisib (1 μM).

(d) Western blots to detect regulators and targets of PI3K signaling pathway in HCC-1806, HCC-1937, SUM-159, MDA-MB-231, MDA-MB-468, BT-549, and HMEC cells.

(e) Western blots show PTEN KO dramatically enhanced p-AKT at both Thr308 and Ser473 sites in HCC-1806 and HCC-1937 cells.

(f-g) PTEN KO led to cell resistance to Alpelisib in HCC-1806 and HCC-1937 cells. IC_{50} denotes half maximal inhibitory concentration.

Supplementary Figure 2. The physicochemical characteristics of ^{68}Ga-pAKTi

(a) Radio labeling rate of ^{68}Ga-pAKTi under different pH condition.

(b) Radio labeling rate of ^{68}Ga-pAKTi at different reaction time.

(c) *In vitro* stability of ^{68}Ga-pAKTi after incubation in PBS or mouse serum for 3 h at room temperature or 37°C respectively.

(d) Retention curves of ^{68}Ga-pAKTi in MDA-MB-231, MDA-MB-468, and BT-549 cells. %AD = percentage administered dose. Data were expressed as mean ± SEM.

(e) Competitive binding curves for half-maximal inhibitory concentration determination of ^{68}Ga-pAKTi in MDA-MB-231, MDA-MB-468, and BT-549 cells, using GDC-0068 as competitive inhibitor.

(f) Blood radioactivity profile of ^{68}Ga-pAKTi. Data were expressed as mean ± SEM.

Supplementary Figure 3. ^{68}Ga-pAKTi PET/CT imaging detects p-AKT *in vivo* and predicts response of triple negative breast cancer to Alpelisib

(a) Tumor weight of HCC-1806, HCC-1937, MDA-MB-231, and MDA-MB-468 tumors after Alpelisib or control treatment. Control (PBS), n = 5; Alpelisib (25 mg/kg), n = 5. Data were presented as Mean ± SEM.

(b-c) The correlation between protein levels of p-AKT^{Thr308} or p-AKT^{Ser473} and the ^{68}Ga-pAKTi uptake (%ID/g) in HCC-1806, HCC-1937, MDA-MB-231, MDA-MB-468 tumors.

(d) Biodistribution of ^{68}Ga-pAKTi in mice bearing HCC-1806, HCC-1937, MDA-MB-231, MDA-MB-468 tumors.

Supplementary Figure 4. ^{68}Ga-pAKTi PET/CT imaging shows high specificity to detect TNBC tumor p-AKT *in vivo*

(a) Design of the *in vivo* blocking experiment.

(b) Representative ^{68}Ga-pAKTi micro-PET/CT images of MDA-MB-468 xenografts with and without GDC-0068 blocking.

(c) Uptake values of ^{68}Ga-pAKTi micro-PET/CT (%ID/g) in the non-blocked and blocked MDA-MB-468 tumors (n = 5).

Supplementary Figure 5. PTEN loss leads to TNBC tumor resistance and enhanced p-AKT upon long-term treatment of Alpelisib

(a) Growth curve of HCC-1937 PTEN WT and HCC-1937 PTEN KO tumors after long-term Alpelisib or vehicle treatment. Vehicle (PBS), Alpelisib (25 mg/kg). (n = 5).

(b) Tumor weight of HCC-1937 PTEN WT and HCC-1937 PTEN KO tumors after long-term Alpelisib or vehicle treatment. Vehicle (PBS), Alpelisib (25 mg/kg). Data were presented as Mean ± SEM.

(c) Representative images of formalin-fixed paraffin-embedded sections obtained from HCC-1806 PTEN WT, HCC-1806 PTEN KO, HCC-1937 PTEN WT, and HCC-1937 PTEN KO tumors stained for Ki67. Bar, 20 μm.

Supplementary Figure 6. The uptake changes of ^{18}F-FDG upon short-term treatment of PI3Kα Inhibitor in PTEN KO TNBC tumors *in vivo*

(a) Representative ^{18}F-FDG PET/CT images of mice bearing HCC-1806 PTEN WT, HCC-1806 PTEN KO, HCC-1937 PTEN WT, and HCC-1937 PTEN KO tumors. 7.4 MBq ^{18}F-FDG was injected via tail vein for each mouse.

(b) Uptake values of ^{18}F-FDG micro-PET/CT (%ID/g) in the HCC-1806 PTEN WT and HCC-1806 PTEN KO tumors (n=5 / group).

(c) Uptake values of ^{18}F-FDG PET/CT (%ID/g) in the HCC-1937 PTEN WT and HCC-1937 PTEN KO tumors (n=5 / group).

Supplementary Figure 7. The p-AKT signaling and tumor responses to Alpelisib in TNBC tumors with PIK3CA-H1047R mutation

(a) Western blots to show PIK3CA-H1047R mutation robustly increased p-AKT in HCC-1806

Vector, HCC-1806 PIK3CA-H1047R, HCC-1937 Vector, and HCC-1937 PIK3CA-H1047R cells.

(b) Body weight of mice bearing HCC-1806 Vector or HCC-1806 PIK3CA-H1047R tumors upon Alpelisib or vehicle treatment (25 mg/kg) (n = 5 / group). Data were shown as Mean ± SEM.

(c) Representative images of formalin-fixed paraffin-embedded sections obtained from HCC-1806 Vector and HCC-1806 PIK3CA-H1047R tumors with vehicle or Alpelisib treatment (25 mg/kg), stained for PTEN, p-AKT^{Thr308}, p-AKT^{Ser473}, and Ki-67. Bar, 20 μm.

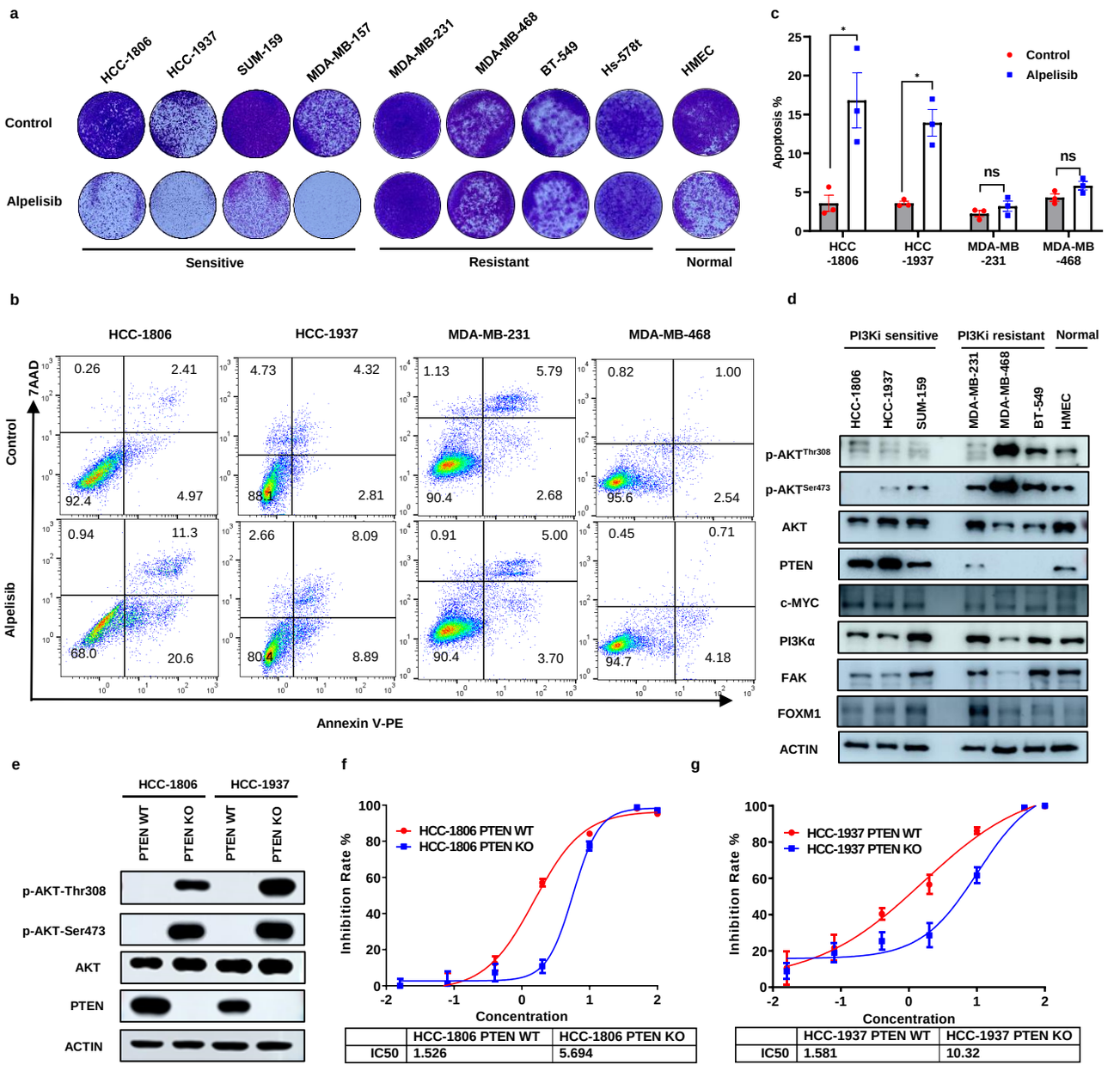
a
HCC-1806
HCC-1937
SUM-159
MDA-MB-157
MDA-MB-231
MDA-MB-468
BT-549
Hs-578t
HMEC
Control
Alpelisib
Sensitive
Resistant
Normal
c
Apoptosis %
Control
Alpelisib
*
*
ns
ns
HCC -1806
HCC -1937
MDA-MB -231
MDA-MB -468
b
HCC-1806
HCC-1937
MDA-MB-231
MDA-MB-468
7AAD
Control
Alpelisib
Annexin V-PE
0.26
2.41
92.4
4.97
4.73
4.32
88.1
2.81
1.13
5.79
90.4
2.68
0.82
1.00
95.6
2.54
0.94
11.3
68.0
20.6
2.66
8.09
80.4
8.89
0.91
5.00
90.4
3.70
0.45
0.71
94.7
4.18
d
PI3Ki sensitive
PI3Ki resistant
Normal
HCC-1806
HCC-1937
SUM-159
MDA-MB-231
MDA-MB-468
BT-549
HMEC
p-AKTThr308
p-AKTSer473
AKT
PTEN
c-MYC
PI3Kα
FAK
FOXM1
ACTIN
e
HCC-1806
HCC-1937
PTEN WT
PTEN KO
PTEN WT
PTEN KO
p-AKT-Thr308
p-AKT-Ser473
AKT
PTEN
ACTIN
f
Inhibition Rate %
HCC-1806 PTEN WT
HCC-1806 PTEN KO
Concentration
HCC-1806 PTEN WT
HCC-1806 PTEN KO
IC50
1.526
5.694
g
Inhibition Rate %
HCC-1937 PTEN WT
HCC-1937 PTEN KO
Concentration
HCC-1937 PTEN WT
HCC-1937 PTEN KO
IC50
1.581
10.32

Supplementary Figure 2

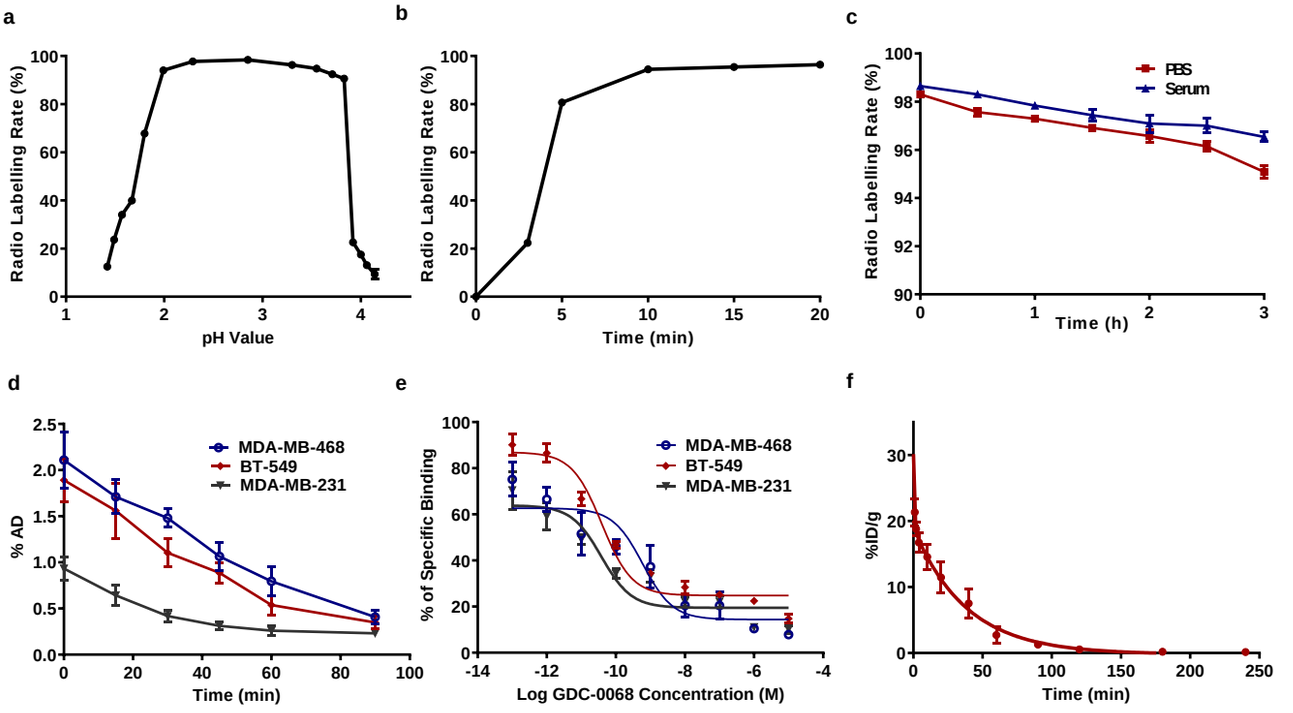

Supplementary Figure 3

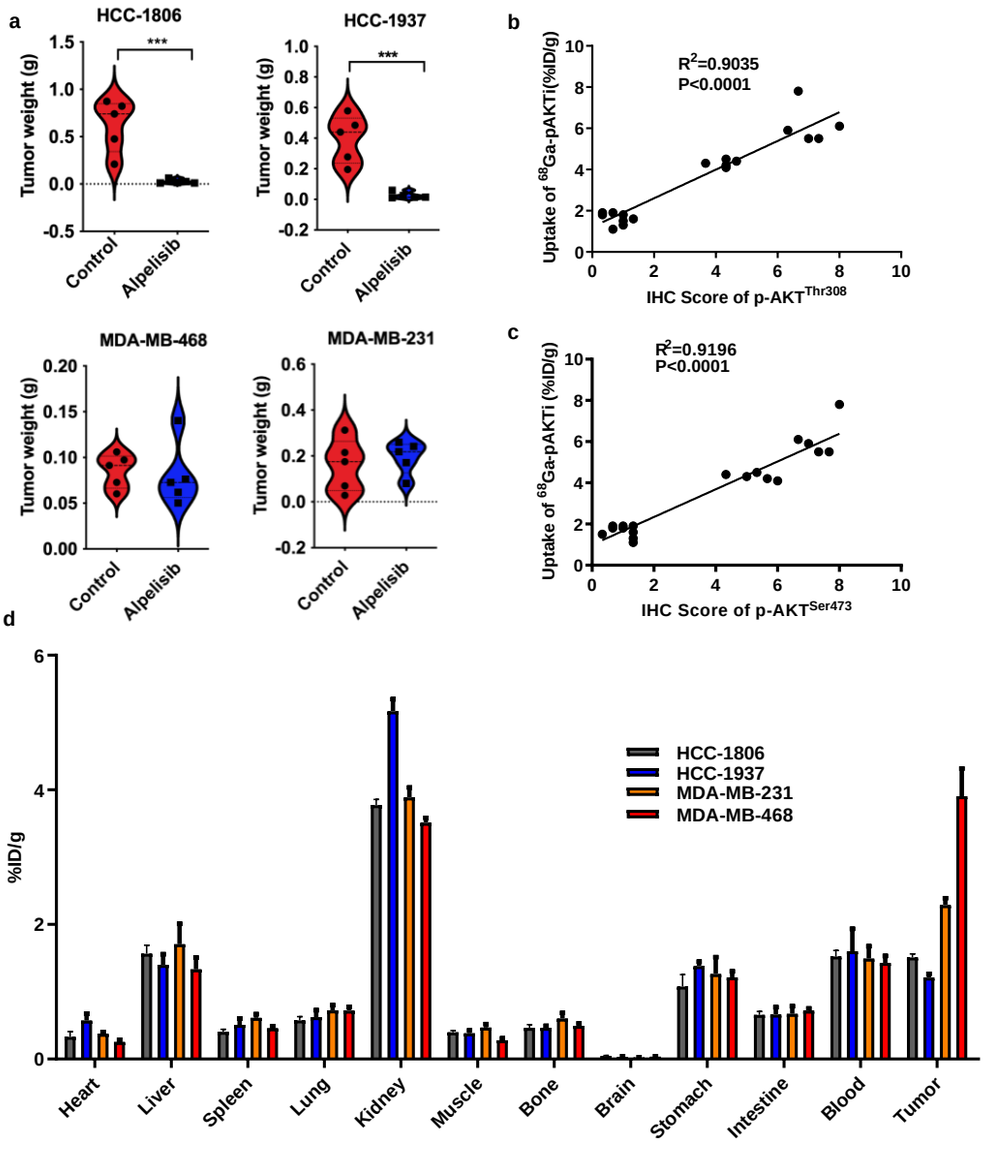

Supplementary Figure 4

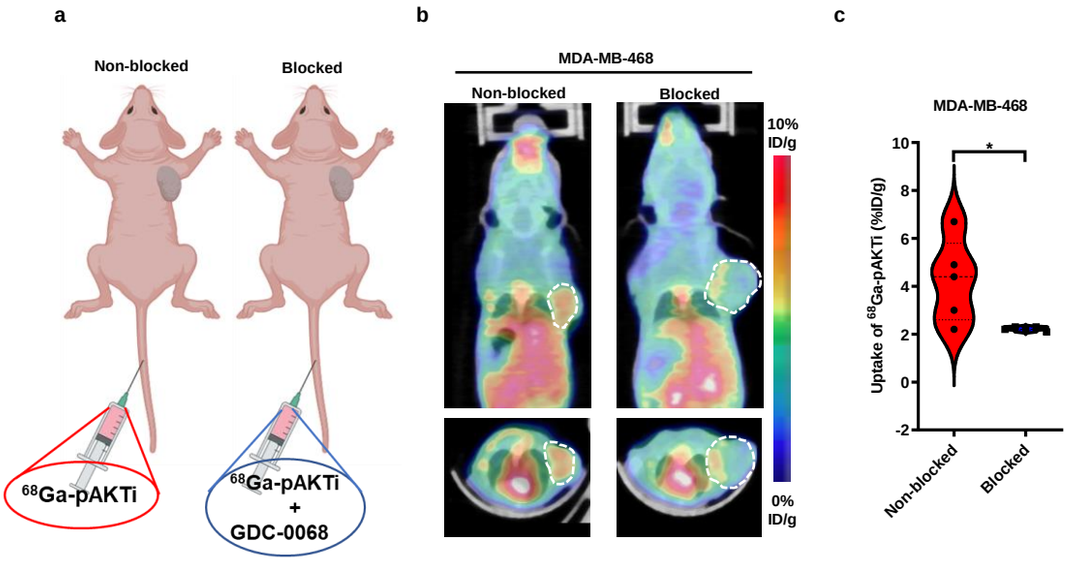

Supplementary Figure 5

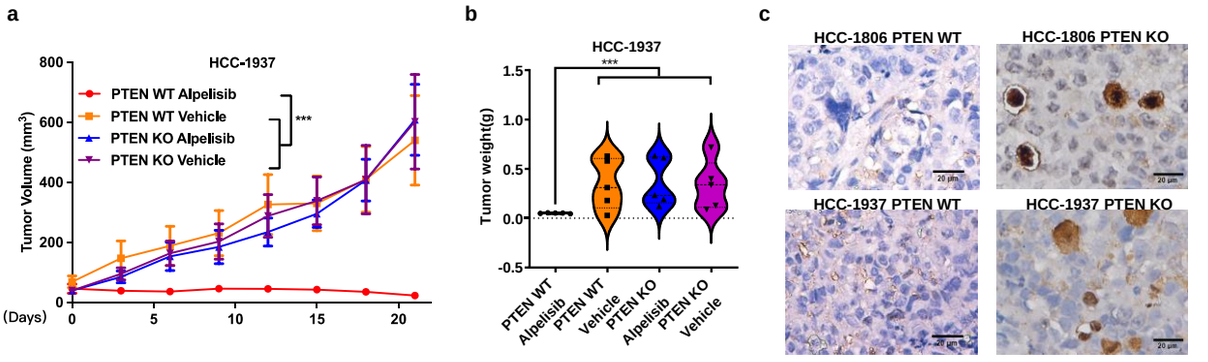

Supplementary Figure 6

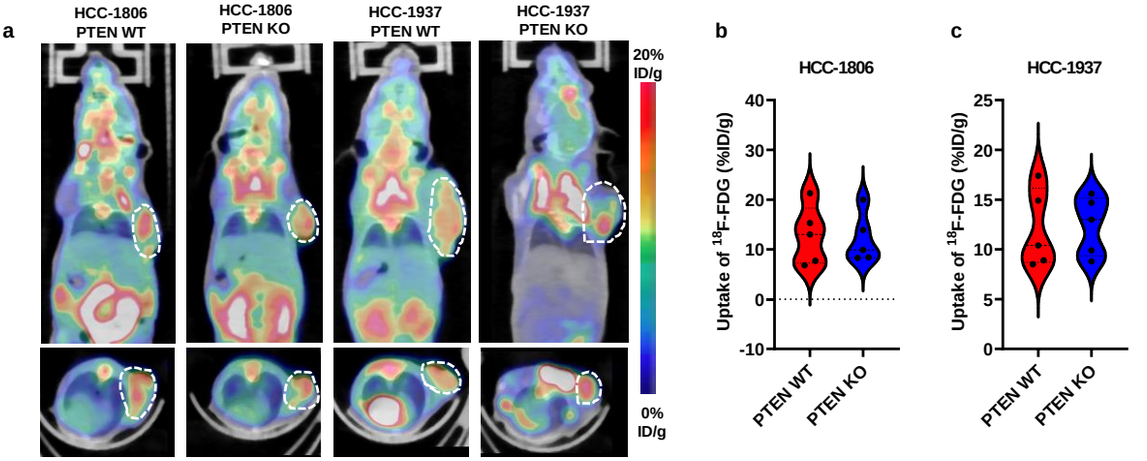

Supplementary Figure 7